Uncertainty of ice-penetrating radar and new Age-Depth profiles at Byrd Ice Core, West Antarctica

Gail Gutowski

Department of Geosciences, University of Texas at Austin, Austin, TX

Charles Jackson, Donald Blankenship, and Duncan Young

Institute for Geophysics, University of Texas at Austin, Austin, TX

————

Abstract.   We present a new depth chronology for ice near Byrd ice core which accounts for uncertainties in ice penetrating radar and ice core dating. Our chronology consists of an ensemble of age-depth profiles representing the physical range of uncertainty associated with prominent radar reflectors in the ice. These profiles are useful for inferring ice strain rates and ice velocities, which are necessary for modeling ice dynamics.

1. Introduction

Understanding ice dynamics and mass balance of ice sheets is important to predict how the Earth's polar regions will respond to global environmental change. While studies of mountain glaciers strongly suggest significant ice depletion in the next century given current global warming trends [*Meier et al.*, 2007], the response of large-scale ice sheets such as Greenland and Antarctica is uncertain. This is largely due to a lack of information about the internal dynamics of these ice sheets.

Ice sheet response to changes in climatic conditions in the past can be useful in evaluating future response. Age-depth relationships from ice cores are one tool available for understanding ice dynamics and accumulation history at particular locations on an ice sheet. More recently, ice-penetrating radar has made it possible to extend age-depth profiles over larger regions of the ice sheet [*Neumann et al.*, 2008, e.g.].

Internal radar horizons encode information about accumulation rates and ice deformation which can be used to determine ice velocities and strain rates. Such a picture of ice dynamics has been lacking in the past; the last report by the Intergovernmental Panel on Climate Change neglected the influence of ice dynamics in its projections of future sea level rise [*Change*, 2007]. Many modeling efforts are underway to fill this gap and will benefit from incorporation of internal radar horizons as a metric for model validation.

However, it is important to understand uncertainty in ice-penetrating radar data and how that uncertainty may affect modeling efforts. The accuracy of dating internal radar horizons depends on uncertainty in radar observations and in ice-core dating. *Eisen et al.* [2004] evaluated this uncertainty for ground-based radar in the top 100 m of the East

Antarctic Ice Sheet. We approach the problem using airborne observations of WAIS near Byrd ice core and consider radar horizons in the top 1300 m of the ice sheet. We use an ice-core derived chronology and a one-dimensional ice flow model to evaluate the uncertainty in airborne ice-penetrating radar observations. We present a resulting ensemble of age-depth profiles, which includes appropriate consideration of uncertainties in both age and depth.

2. Data

2.1. Radar Data

Ice-penetrating radar-echo sounding data was obtained in December 2004 as part of the Airborne Geophysical Survey of the Amundsen Sea Embayment (AGASEA) project [*Holt et al.*, 2006]. The radar line passed 870 m from the Byrd ice core site while the plane was traveling 67 m/s at an elevation of 550 m above the ice surface. The data includes two-way travel times (the time it takes for a radar pulse to be transmitted, reflect off a layer, and return to the receiver) in microseconds, which were collected with a 15 MHz bandwidth. We use ten strong radar horizons that were hand-traced at the University of Texas Institute for Geophysics using the seismic imaging software *GeoFrame*. The horizons were selected for their prominence, which ensured that they could be traced through the domain. The ten horizons of interest are shown in Figure /refradargram.

Radar reflection horizons provide an avenue for developing an understanding of ice dynamics. Each year, snow accumulates on the surface of the ice sheet. The physical properties of this snow contain information about climatic conditions at the time of deposition; for instance, the oxygen isotope, $\delta^{18}O$, can be used as a proxy for temperature. Over time, the surface layer is covered with the accumulation of subsequent years and

becomes buried in the ice column. Differences in chemical composition of these deposited layers lead to variations in electrical conductivity observed by the radar as horizons, or horizontal layers. We therefore interpret the radar horizons as isochronous [*Eisen et al.*, 2004].

2.2. Byrd ice core chronology

The Byrd ice core was drilled in 1968 and was the first in Antarctica to extend to bedrock [*Gow et al.*, 1968]. Damage to the ice core above 88 m prohibited the traditional approach of annual layer counting, so the chronology was instead determined by locating the 1259 AD volcanic horizon at 97.8 m below the 1968 ice surface. Below 88 m, the electrical conductivity method (ECM) was used to date the ice core [*Hammer et al.*, 1994]. The ECM method measures variations in electrical conductivity. Between 300 m and 900 m, brittle ice precluded sufficient ECM measurements. *Hammer et al.* [1994] instead fit the chronology with three piecewise linear functions. The resulting layer-thickness profile was integrated from surface to depth to obtain an age-depth relationship for the length of the ice core.

Hammer et al. [1997] presented a volcanic chronology based on this previously derived timescale in which volcanic events were matched to peaks in electrical conductivity. The chronology includes dated volcanic events that cover an age range from 709 BP to more than 18000 BP, corresponding to depths ranging from 97.8 m to 1890 m below the 1968 surface of the Byrd ice core.

Ice density data as a function of depth were obtained from the original analysis of the ice core [*Gow et al.*, 1968]. The data were used to account for the varying density of ice

in the upper part of the ice sheet. The result was used to apply a constant firn correction to the ice thickness at Byrd ice core.

3. Sources of Uncertainty

There are many sources of uncertainty inherent to the way in which data is collected, analyzed, and understood. We have included the following sources of uncertainty.

3.1. Radar Uncertainty

Radar horizons, surfaces of constant two-way travel time (TWTT), are hand-traced using seismic interpretation software. This allows a user to select strong reflectors from a radargram and trace them along a radar line. However, there is a limit to the accuracy of tracking a single phase of a radar reflection. The vertical accuracy depends on the resolution of the sampling rate of the radar transmitter as well as considerations of noise. For high sampling rates, the uncertainty in phase selection is typically $\frac{\lambda}{4}$, but can be as accurate as $\frac{\lambda}{2}$ for data with high signal-to-noise where λ is the wavelength of the electromagnetic pulse. The sampling rate for the data used here varies from 5 ns to 20 ns. To be conservative, we assume a 10 ns resolution when tracking the phase of reflections from the surface of the ice sheet and from each internal layer. We treat the surface and internal layers separately in this instance.

To convert TWTT uncertainty into units of depth, we scale the time by the velocity of electromagnetic wave propagation in the medium. The pulse traveled from the aircraft to the ice sheet surface with velocity, c, the speed of light, and then slowed to the velocity of electromagnetic wave propagation in ice, which we take to be $c_i = 1.69$ x 10^8 m/s before reaching the internal layers and reflecting back. The corresponding 1σ uncertainty is σ_{surf}

~0.3 m for the surface reflector and $\sigma_{lay} \sim 0.17$ m for each of the internal layers, assuming the uncertainty is gaussian.

The uncertainty associated with picking the elevation of the surface is considered a systematic error because the same surface elevation will be used to normalize all of the internal layers. The TWTT uncertainty of each of the internal layers is applied randomly because each of the individual layers need not have the same uncertainty. This is because the reflection from each layer need not have the same phase with respect to the sampling rate. To account for this, we assume the TWTT to be normally distributed and sample randomly from this distribution for each of the internal layers independently.

The finite bandwidth of the data means that even an infinitesimally thin layer of ice will appear in the survey to have a finite width. Our data uses a pulse bandwidth of 15 MHz. This translates to a 1σ depth uncertainty of 5.63 m, obtained from considering both the bandwidth frequency and the velocity of electromagnetic radiation in ice. This uncertainty is applied as a random, normally distributed error in the depth of each of our selected layers.

3.2. Age Uncertainty

Each year, fresh snow accumulates on top of the ice sheet, burying the previous season?s snowfall. As layers of ice descend into the ice sheet, they become thinner because air is squeezed out and gravity compacts the ice. This thinning makes it increasingly difficult to distinguish one layer from another at depth. In shallow regions, it is possible to count layers by eye to determine the age of near-surface isochrones; however, this is harder to do deep in the ice sheet. The uncertainty associated with determining ages for ice layers is therefore a function of depth.

The upper part of the original 1968 Byrd ice core was too damaged to count annual layers. However, in 1989, a shallow core dubbed NBY89 was drilled nearby which enabled [*Langway et al.*, 1994] to complete a chronology for the top 164 m of the core. Using the ECM method [1], they matched 3 volcanic events to the original ice core with an uncertainty of $\sigma_{age} = \pm 2$ yr for the upper 1360 a of the ice core.

Isotopic dating is common among ice core chronologies. Landmark events for concentrations of Beryllium-10, methane, and fluorine (to name a few) are matched to chemical analyses of the ice [*Schwander et al.*, 2001] at different points in time. Accepted dates for these events are then mapped onto the ice core.

We adopt the following estimates of uncertainty to accompany the isotopic dating, though no comprehensive review of uncertainty from these methods is available. The end of the Younger Dryas period is correlated between the GRIP and Byrd ice cores using CH_4. This method indicates an uncertainty of roughly $\sigma_{age} = \pm 150$ yr for the period between 1360 a and 11.5 ka [*Blunier et al.*, 1998; *Schwander et al.*, 2001]. This incorporates uncertainty in the δage estimate on the GRIP and Byrd cores (± 100 yr) as well as the CH_4 match between the GRIP/Byrd (± 100 yr). For the period between 11500 a and 17320, we adopt an uncertainty of $\sigma_{age} = \pm 300$ yr [*Schwander et al.*, 2001]. This value is the result of stratigraphic layer counting near a prominent fluoride peak at Byrd station, tuned by matching CH_4 during the Younger Dryas period.

For layers older than 17320 a, we assume $\sigma_{age} = 2$ ka based on U/Th dating of the Laschamp geomagnetic excursion [*Schramm et al.*, 2000]. Note that we include this uncertainty for completeness; the ten radar horizons of interest in this analysis are believed to be younger than 17320 a.

Table 1 summarizes the uncertainty we assign to observed ages as a function of depth.

4. Method

We use an ice flow model adapted from *Morland* [2009] to determine the age of internal layers near the Byrd ice core drilling site in Antarctica. The simple flow model has the following form:

$$\frac{\bar{z}}{h_0} = \frac{1}{1-r}[1 - exp(-s\bar{t})]$$

$$\bar{z} = h_0 - z$$

$$r = \frac{b}{q} \tag{1}$$

$$s = s_d s_0$$

where depth, $\bar{z}$, is defined to be 0 at the base, $h_0 = 2164$ m is the depth at the ice sheet surface, b is basal melting rate, q is the accumulation rate, and $\bar{t}$ is the age corresponding to $\bar{z}$. The optimum constant strain rate, s, is used to achieve reasonable correlations between the model and observations; s_0 is the initial strain rate and s_d =0.722 for the Byrd ice core. The model assumes isostatic equilibrium, constant ice density, uniform strain rate in z, and $r < 1$ (i.e. nonnegative mass balance in the ice column). Note that it is difficult to know accumulation rate on its own due to layer thinning within the ice column. As such, we consider layer thickness instead of layer accumulation because it can be physically measured using the techniques described previously. Further, while depth in the model, $\bar{z}$, is defined so that $\bar{z}$(base) = 0, the following analysis is discussed in terms of depth z, where $z(surface) = 0$.

We use the flow model to invert for layer thickness as a function of depth, q, and strain scale factor, s, using an observed age-depth relationship. We use the resulting parameters to evaluate the age of ten prominent radar horizons. The inversion is done using a Markov Chain Monte Carlo technique known as the Metropolis. We use a stepwise function to describe layer thickness, breaking it into four depth regimes:

$$z = \begin{cases} z_1 & \text{z} < 150\text{m} \\ z_2 & 150\text{m} \leq \text{z} < 1024m \text{ m} \\ z_3 & 1024\text{m} \leq \text{z} < 1294\text{m} \\ z_4 & \text{z} \geq 1292\text{m} \end{cases}$$

These regimes were chosen based on a linear piecewise function of layer thickness developed by *Hammer et al.* [1994] in which shifts are seen at the above transition points.

The Metropolis algorithm utilizes prior knowledge about the model parameters (accumulation and strain scale factor) to develop a joint posterior distribution of the parameters. We use truncated uniform priors on all parameters, allowing them to take on values within a physically reasonable range: layer thickness is allowed to vary between 0 cm/a and 30 cm/a, while the strain scale factor may take values between 0 and 1.7. The model is initialized using random parameter values within these ranges.

At each model step, we evaluate the age model at every point in the ice column based on proposed sets of parameters. An associated cost is calculated as a measure of the model/data misfit for each proposal. The log likelihood is described in equation 2:

$$loglikelihood = \frac{(Age_{model} - Age_{obs})^2}{(\sigma_{obs})^2} \tag{2}$$

where Age_{model} is evaluation of the *Morland* [2009] ice flow model for a given accumulation and strain scale factor. Age_{obs} and σ_{obs} come from the volcanic age-depth function and we allow for the aforementioned uncertainty in Age_{obs} (see Table 1)to loosen the constraint on the cost function. At each iteration the algorithm makes a decision about whether or not to accept the combination of parameters based on the cost: if the cost of the nth iteration is less than the cost of the *(n-1)*th iteration, the set of parameters is accepted. This means that the nth set of parameters is a better fit to the data, because the cost has decreased. If the cost of the current nth iteration is greater than the cost of the *(n-1)*th iteration, the set of parameters is accepted with probability $exp[-\frac{cost_n - cost_{n-1}}{2}]$, the Metropolis probability. The algorithm continues on a random walk through parameter space, minimizing cost at each step.

We use the Metropolis algorithm to generate a large number of age-depth distributions that together describe the probability of the age of a radar horizon at a given depth based on knowledge about ice flow and layer thickness. We generate 20000 sets of parameters (accumulation and strain rate) that characterize physically reasonable models of age-depth. Age uncertainty is taken to be the variance in age at a given depth.

Uncertainty in the radar-derived depth of each horizon is considered next. To find the radar sampling rate uncertainties, we draw a single value from the probability distribution for the surface reflector, described by σ_{surf}. We then randomly sample ten values from a probability distribution described by σ_{lay}, resulting in a radar sampling rate for each of the horizons of interest. The bandwidth uncertainty is found in the same fashion as the sampling rate error for the layers. The bandwidth and sampling rate uncertainty vectors are summed in quadrature to arrive at a total radar uncertainty for each radar horizon.

We also add a correction for firn density and account for additional accumulation between 1968 (when the core was drilled) and 2004 (when the radar line was flown) assuming a constant accumulation rate of 11 cm/a *Hammer et al.* [1994].

This process is repeated 20000 times to build a probability distribution describing the depth of each radar horizon. For each sample in depth probability distribution (20000 in all), we randomly sample an age-depth model from the ensemble generated previously. The selected model is evaluated at each of the ten radar horizon depths for a given sample. The result is an ensemble of 20000 age-depth profiles for the radar horizons of interest which incorporate uncertainty in both age and depth.

5. Results

Figure a shows the distribution of modeled depths associated with each ice layer of interest from radar observations near Byrd Station, West Antarctica. The spread in the distribution is indicative of uncertainty due to observational methods. Table 2 shows the standard deviation of depth for each of the ten chosen layers, assuming the errors to be gaussian. See Section 3.2 for a full discussion of the sources of uncertainty included in this analysis. The uncertainty in each layer depth is more or less constant with depth. However, deeper in the ice sheet, ∼1250 m below the surface, radar horizons 7/8 and 9/10 are observed as being distinct in the radar TWTT are consistent within uncertainty with being from the same deposition event or isochrone.

The corresponding age distributions are shown in Figure b and again assume gaussian errors. Table 2 shows the mean and standard deviation for each peak. Due to increased uncertainty in ice core dating, age uncertainty increases with depth. As with depth, layers at X m and X m are consistent with originating during the same period. This ambiguity

makes it clear that robust uncertainty quantification is critical for the interpretation of internal layers; dynamic analyses require that radar horizons be distinguished in order to obtain a time-dependent profile of ice flow.

Figure shows an ensemble of modeled age-depth distributions for the ten picked radar layers. The distributions are trained on the observed volcanic record at Byrd Station, allowing for uncertainties in both depth and age. Note that both systematic and random sources of uncertainty are included. Crossing lines indicate that random uncertainty plays a significant part in the age-depth distribution of ice layers at Byrd Station. Spread between ensembles that do not cross is representative of systematic uncertainties in the model.

As described in Section 4, the model is based on five parameters: layer thickness parameters in four depth regimes and a ratio of surface to bed ice velocity. Figure shows the distributions of the layer thickness parameters, which are used as a proxy for accumulation in the model. As expected due to layer thinning with depth, mean layer thickness decreases with depth. The modeled layer thickness is consistent with layer thickness at the Western Divide determined by [*Neumann et al.*, 2008] above 1294 m; Table shows a comparison between the two. We expect layer thickness to be at a maximum at the divide and therefore reasonable values at Byrd Station should be less than those at the divide. Our modeled layer thickness below 1294 m is larger than shallower modeled thicknesses and greatly exceeds the layer thickness at the divide at this depth. However, this depth corresponds to only the deepest radar horizon of interest, so it should not affect the result.

6. Discussion and Conclusion

Uncertainty associated with two-way travel time in airborne ice-penetrating radar surveys of Antarctica is not thoroughly understood. We seek to quantify that uncertainty and its affect on depth and age uncertainties near Byrd Station, West Antarctica. Our approach employs a simple ice flow model and basic parameter assumptions which we will improve upon in the future. The ice flow model used in this analysis relies heavily on the function of ice accumulation chosen. Here we have chosen to simplify our approach by using layer thickness as a proxy for accumulation. By proposing constant layer thickness in each of four depth regimes, we further approximate accumulation with a discontinuous function. Our depth regimes were selected based on an approximation by *Hammer et al.* [1994]. While a useful tool, a continuous function of accumulation will be included in the future.

Another assumption in our analysis is the choice of ice flow model. We use a simple model developed for the Byrd ice core by *Morland* [2009]. To further simplify the model, we assume no basal melting, however this is a poor assumption based on the amount of liquid water found at the base of the ice sheet when the core was drilled to bedrock [*Gow et al.*, 1968]. Geothermal flux derived from a borehole temperature profile was estimated to be 75 mW m^{-2} by *Gow et al.* [1968]. Additionally, the model assumes only vertical strain, ignoring potentially important longitudinal contributions to ice flow. Ice near Byrd Station is flowing at $v_{surf} \sim 11$ m/a, about 0.5 km since the Byrd ice core was drilled, so it is important to include horizontal components in future analyses [*Bindschadler et al.*, 1997]. The wide-ranging nature of continuous radar observations make radar data ideal

for studying these kinds of longitudinal effects, which will be included with more complex models of ice flow in the future.

Our analysis revealed that when uncertainty is accounted for, radar horizons that appear at first to be distinct events in the ice column, may in fact be from the same ice deposition event at the surface. This issue is further complicated by the role played by human interpretation in the process. Figure /refradargram shows Horizons 9 and 10 to be in virtually the same position through part of the domain before diverging at the horizontal position where our data was taken. This divergence may be attributed to discontinuity in the appearance of the layers and the presence of a reflection hyperbole from the ice sheet surface. Steps have been taken to correct for potential error in cases such as this, including independent horizon tracking by multiple people as a mode of comparison. This precaution instituted after this data was collected and interpreted and so has not been included in this analysis. However, we have shown that with careful consideration of uncertainty, we are able to account for the error introduced by the difficulty of interpreting horizons such as Horizons 9 and 10 in this study. Though Horizons 9 and 10 were originally traced as distinct, our analysis has shown that they perhaps should be interpreted as the same isochronous horizon, a conclusion that is further supported by visual inspection of the radargram in Figure /refradargram.

7. Draft notes

1. Covariance

2. Map of Byrd

3. Full table of age-depth profiles ensemble

4. What results to include in abstract?

Notes

1. The Electrical Conductivity Method (ECM) is another approach to dating ice. It involves measuring the conductivity of ice at different depths [*Hammer et al.*, 1994]. This conductivity is associated with the composition of the ice, characterized by its acidity level. Layers of ash embedded in the ice, for example, will have a distinct conductivity. The ECM method is particularly useful in deep parts of the ice column where it is difficult to otherwise distinguish isochronous layers due to layer thinning.

References

Bindschadler, R., X. Chen, and P. Vornberger, Surface velocity and strain rates at the onset of ice stream d, west antarctica, *Antarctic Journal of the United States*, *32*(5), 41–43, 1997.

Blunier, T., et al., Asynchrony of Antarctic and Greenland climate change during the last glacial period, *Nature*, *394*, 739–743, doi:10.1038/29447, 1998.

Change, I., Climate change 2007: The physical science basis, *Agenda*, *6*, 07, 2007.

Eisen, O., U. Nixdorf, F. Wilhelms, and H. Miller, Age estimates of isochronous reflection horizons by combining ice core, survey, and synthetic radar data, *Journal of Geophysical Research (Solid Earth)*, *109*, B04106, doi:10.1029/2003JB002858, 2004.

Gow, A. J., H. T. Ueda, and D. E. Garfield, Antarctic Ice Sheet: Preliminary Results of First Core Hole to Bedrock, *Science*, *161*, 1011–1013, doi:10.1126/science.161.3845.1011, 1968.

Hammer, C., H. Clausen, and C. Langway, 50,000 years of recorded global volcanism, *Climatic Change*, *35*(1), 1–15, 1997.

Hammer, C. U., H. B. Clausen, and C. C. Langway, Jr., Electrical conductivity method (ECM) stratigraphic dating of the Byrd Station ice core, Antarctica, *Annals of Glaciol-*

ogy, *20*, 115–120, 1994.

Holt, J. W., D. D. Blankenship, D. L. Morse, D. A. Young, M. E. Peters, S. D. Kempf,
T. G. Richter, D. G. Vaughan, and H. F. J. Corr, New boundary conditions for the
West Antarctic Ice Sheet: Subglacial topography of the Thwaites and Smith glacier
catchments, *Geophys. Res. Lett.,* , *33*, L09502, doi:10.1029/2005GL025561, 2006.

Langway, C. C., Jr., K. Osada, H. B. Clausen, C. U. Hammer, H. Shoji, and A. Mi-
tani, New chemical stratigraphy over the last millennium for Byrd Station, Antarc-
tica, *Tellus Series B Chemical and Physical Meteorology B*, *46*, 40, doi:10.1034/j.1600-
0889.1994.00004.x, 1994.

Meier, M., M. Dyurgerov, U. Rick, S. O'Neel, W. Pfeffer, R. Anderson, S. Anderson,
and A. Glazovsky, Glaciers dominate eustatic sea-level rise in the 21st century, *Science*,
317(5841), 1064, 2007.

Morland, L. W., Age-depth correlation, grain growth and dislocation-density evolution, for
three ice cores, *Journal of Glaciology*, *55*, 345–352, doi:10.3189/002214309788608723,
2009.

Neumann, T. A., H. Conway, S. F. Price, E. D. Waddington, G. A. Catania, and D. L.
Morse, Holocene accumulation and ice sheet dynamics in central West Antarctica, *Jour-
nal of Geophysical Research (Earth Surface)*, *113*, F02018, doi:10.1029/2007JF000764,
2008.

Schramm, A., M. Stein, and S. L. Goldstein, Calibration of the ^{14}C time scale to ¿ 40
ka by ^{234}U-^{230}Th dating of Lake Lisan sediments (last glacial Dead Sea), *Earth and
Planetary Science Letters*, *175*, 27–40, doi:10.1016/S0012-821X(99)00279-4, 2000.

```
Byrdlayers_paper.eps
```

Figure 1: Radargram of the area observed near Byrd ice core highlighting the ten radar horizons analyzed. The arrow on top of the figure indicates the location of the horizontal position of radar observations used. Our analysis shows that Horizons 7 and 8 and Horizons 9 and 10 are consistent within uncertainty to belonging to the same isochrone, though they appear distinct in the radargram. This emphasizes the importance of uncertainty quantification in interpretation of these horizons.

Schwander, J., J. Jouzel, C. U. Hammer, J.-R. Petit, R. Udisti, and E. Wolff, A tentative chronology for the EPICA Dome Concordia ice core, *Geophys. Res. Lett.,* , *28*, 4243–4246, doi:10.1029/2000GL011981, 2001.

agedepthhist_morland.eps

Figure 2: a) Histogram of modeled water-equivalent ice depth for each of ten prominent radar horizons observed using airborne radar near Byrd Station, West Antarctica. The width of each distribution is the result of uncertainties arising from the method of radar collection. b) Similar histogram in terms of age (ka). Age uncertainty comes from approximate uncertainty in ice core dating techniques.

agedepth_metrop.eps

Figure 3: Ensemble of modeled age-depth profiles near Byrd ice core. Black dots represent dated volcanic events from the Byrd ice core record *Hammer et al.* [1994]. Each line represents a set of parameters that describe the observed data within uncertainty. (See Section 4.)

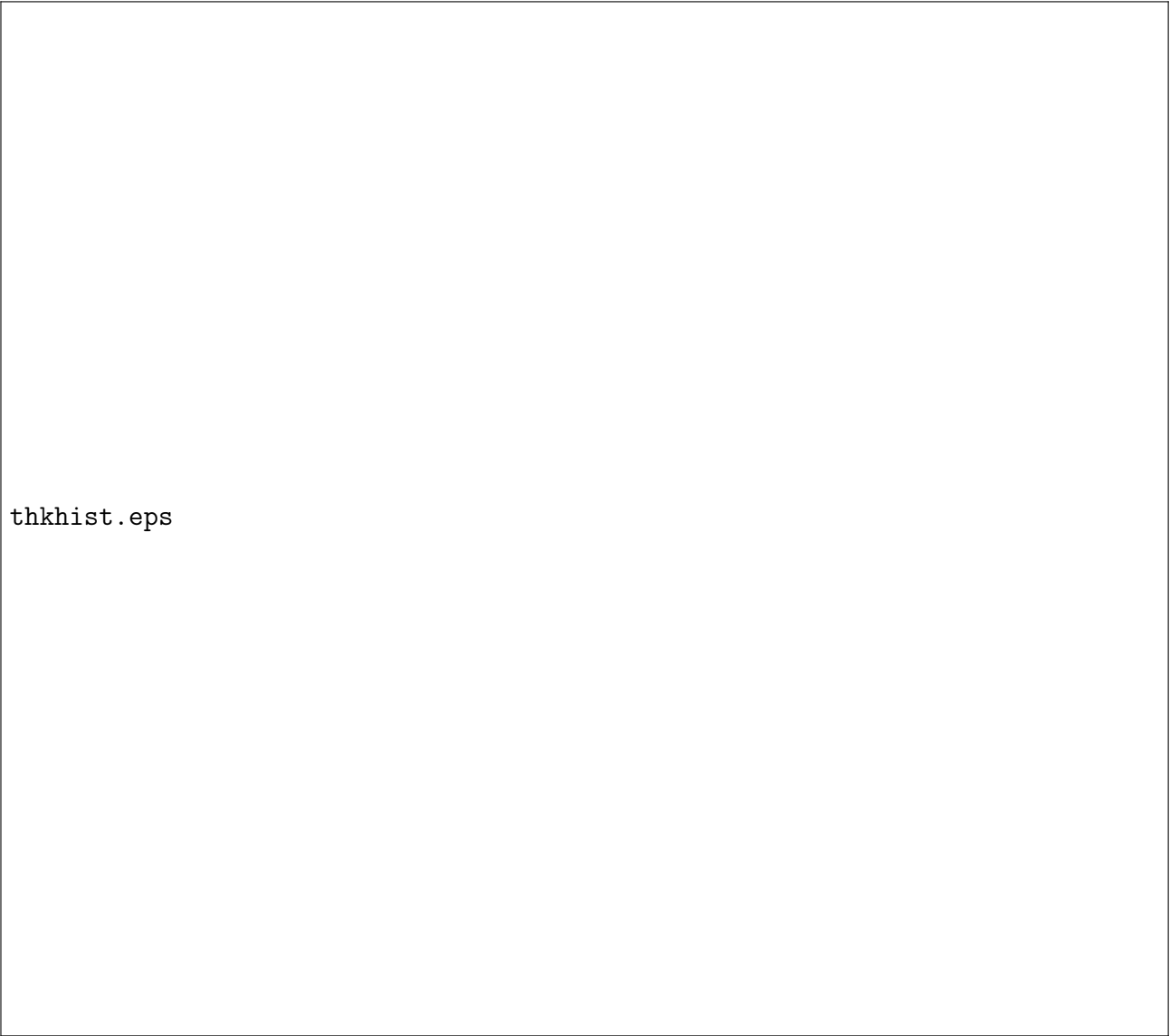| Depth Range (m)	Layer thickness at Divide (m)	Median Layer thickness at Byrd (m)	1σ Uncertainty (m
d < 150	∼0.27	0.10	0.018
150 < d < 1024	∼ 0.14 - 0.27	0.13	0.031
1024 < d < 1294	∼ 0.08 - 0.14	0.16	0.021
d > 1294 <	∼ 0.08 - 0.20	0.19	0.026

Table 1: Comparison between layer thickness at the Western Divide between the Ross and Amundson Seas [*Neumann et al.*, 2008] and modeled here at Byrd Station. Maximum layer thickness occurs at the divide, so layer thicknesses at Byrd Station are expected to be less, but comparable, at Byrd Station. We find that layer thickness at Byrd is the same as layer thickness at the Divide to within uncertainty, implying that our model is overestimating layer thickness. This is especially the case at depth, where we expect layer thinning to decrease the thickness of deeper layers due to increased strain.

hor_agedepth_morland.eps

Figure 4: Age-depth profile of ten prominent radar horizons compared to an observed volcanic age-depth profile of the Byrd ice core. The depth and age of each radar horizon are randomly sampled within uncertainty to obtain an ensemble of possible values for that horizon.

Age (a)	1σ Uncertainty (a)	Method of Dating
Age < 1360	± 2	ECM method on a shallow follow-up ice core, NBY89 from [*Langway et al.*, 1994]
1360 ≥ Age > 11500	± 150	end of Younger Dryas period and ^{10}Be peak][*Blunier et al.*, 1998]
11500 ≥ Age > 17320	± 300	significant volcanic event "Old Faithful" from *Hammer et al.* [1994]
Age ≥ 17320	± 2000	U/Th dating of Laschamp geomagnatic excursion [*Schramm et al.*, 2000]

Table 2: Uncertainty in Byrd ice core chronology Age uncertainty is considered to be gaussian with standard deviation from a variety of age reference points.

```
thkhist.eps
```

Figure 5: Modeled layer thickness in each of four depth regimes near Byrd Station, West Antarctica. The model overestimates layer thickness, particularly in deeper regimes.

TWTT (us)	Depth (m)			Age (a)		
	Mean	Median	Std Dev	Mean	Median	Std Dev
6.02	167.6	167.6	1.185	1195.	1195.	10
6.775	231.4	231.4	1.173	1771.	1772.	20
7.18	265.6	265.6	1.172	2098.	2097.	30
8.94	414.4	414.4	1.184	3505.	3498.	73
9.9402	499.6	499.6	1.187	4363.	4357.	100
11.1	596.9	596.9	1.173	5444.	5437.	134
12.78	738.8	738.8	1.171	7119.	7107.	186
13.02	759.1	759.1	1.170	7354.	7342.	194
18.92	1257.7	1257.7	1.175	16222.	16306.	881
19.0205	1266.2	1266.2	1.172	16399.	16498.	912

Table 3: Depth and age mean, median, and uncertainty for ten strong radar reflectors near Byrd Station, West Antarctica. The radar two-way travel time (TWTT) is given in column 1.